



UNIVERSITY OF LEEDS

This is a repository copy of *The preferential heterodimerization of human small heat shock proteins HSPB1 and HSPB6 is dictated by the N-terminal domain.*

White Rose Research Online URL for this paper:

<http://eprints.whiterose.ac.uk/110584/>

Version: Accepted Version

Article:

Heirbaut, M, Lermyte, F, Martin, EM et al. (5 more authors) (2016) The preferential heterodimerization of human small heat shock proteins HSPB1 and HSPB6 is dictated by the N-terminal domain. *Archives of Biochemistry and Biophysics*, 610. pp. 41-50. ISSN 0003-9861

<https://doi.org/10.1016/j.abb.2016.10.002>

© 2016, Elsevier. Licensed under the Creative Commons Attribution-NonCommercial-NoDerivatives 4.0 International
<http://creativecommons.org/licenses/by-nc-nd/4.0/>

Reuse

Unless indicated otherwise, fulltext items are protected by copyright with all rights reserved. The copyright exception in section 29 of the Copyright, Designs and Patents Act 1988 allows the making of a single copy solely for the purpose of non-commercial research or private study within the limits of fair dealing. The publisher or other rights-holder may allow further reproduction and re-use of this version - refer to the White Rose Research Online record for this item. Where records identify the publisher as the copyright holder, users can verify any specific terms of use on the publisher's website.

Takedown

If you consider content in White Rose Research Online to be in breach of UK law, please notify us by emailing eprints@whiterose.ac.uk including the URL of the record and the reason for the withdrawal request.

The preferential heterodimerization of human small heat shock proteins HSPB1 and HSPB6 is dictated by the N-terminal domain

Michelle Heirbaut^a, Frederik Lermyte^{b,c}, Esther M. Martin^{b,1}, Steven Beelen^a, Tim Verschueren^b, Frank Sobott^{b,1}, Sergei V. Strelkov^{a,*}, Stephen D. Weeks^{a,*}

^a Laboratory for Biocrystallography, Dept. of Pharmaceutical and Pharmacological Sciences, KU Leuven, Belgium

^b Biomolecular and Analytical Mass Spectrometry Group, Dept. of Chemistry, University of Antwerp, Belgium

^c Centre for Proteomics, University of Antwerp, Belgium

* To whom correspondence should be addressed:

Sergei V. Strelkov, Laboratory for Biocrystallography, Department of Pharmaceutical and Pharmacological Sciences, Herestraat 49 box 822, B-3000 Leuven, Belgium, Tel: +32 16330845, Fax: +32 16323469, e-mail: sergei.strelkov@kuleuven.be,

Stephen D. Weeks, Laboratory for Biocrystallography, Department of Pharmaceutical and Pharmacological Sciences, Herestraat 49 box 822, B-3000 Leuven, Belgium, Tel: +32 16377204, Fax: +32 16323469, e-mail: stephen.weeks@kuleuven.be

Abstract

Small heat shock proteins are ATP-independent molecular chaperones. Their function is to bind partially unfolded proteins under stress conditions. *In vivo*, members of this chaperone family are known to preferentially assemble together forming large, polydisperse heterooligomers. The exact molecular mechanisms that drive specific heteroassociation are currently unknown. Here we study the oligomers formed between human HSPB1 and HSPB6. Using small-angle X-ray scattering we could characterize two distinct heterooligomeric species present in solution. By employing native mass spectrometry we show that such assemblies are formed purely from heterodimeric building blocks, in line with earlier cross-linking studies. Crucially, a detailed analysis of truncation variants reveals that the preferential association between these two sHSPs is solely mediated by their disordered N-terminal domains.

Keywords: HSP20; HSP27; heterooligomers; native mass spectrometry; chaperone, small-angle x-ray scattering

Abbreviations: sHSP(s), small heat shock proteins; MS, mass spectrometry; SDS-PAGE, sodium dodecyl sulfate polyacrylamide gel electrophoresis; yADH, yeast alcohol dehydrogenase; HEWL, hen egg white lysozyme; DTT, dithiothreitol; ACD, α -crystallin domain; SAXS, small-angle X-ray scattering; SEC, size-exclusion chromatography; NTD, N-terminal domain; CTD, C-terminal domain; SUMO, small ubiquitin modifier

¹ Present addresses:

Astbury Centre for Structural Molecular Biology, University of Leeds, Leeds LS2 9JT, United Kingdom
School of Molecular and Cellular Biology, University of Leeds, LS2 9JT, United Kingdom

1. Introduction

Small heat shock proteins (sHSPs) are an important family of chaperones involved in the protein quality control network [1,2]. Functioning in a fully ATP-independent manner, sHSPs detect and capture partially unfolded protein species, maintaining such entities in a soluble state [3,4]. Although sHSPs have a low monomeric molecular weight (typically around 20kDa), the majority of members of this family form high molecular weight polydisperse oligomers that demonstrate rapid subunit turnover [3,5]. Adding to this structural complexity it is also recognized that sHSP orthologues within an organism can form heterooligomers [6–8]. The differential structure and activity of such entities though is poorly understood.

Humans encode ten sHSP homologues [9], several of which are known to form heterooligomers [10,11]. The best characterized heteroassembly is α -crystallin, a complex comprised of a 3:1 ratio of α A- and α B-crystallin [12,13]. Although present in this proportion in most vertebrate lenses, *in vitro* these two sHSPs form mixed oligomers with subunit ratios that reflect the amount of each used [14,15]. Contrasting with this behavior, certain sHSPs form heterooligomers that are always composed of a fixed proportion of the constituent chains. For instance when co-expressed HSPB2 and HSPB3 form heterocomplexes containing the respective sHSPs in a strict 3:1 ratio [16].

In this study we focus on the complex formed between human HSPB1 and HSPB6. These two sHSPs are both highly expressed in muscle tissue, alongside HSPB2 and HSPB5 [17]. Indeed, HSPB1 and HSPB6 were originally identified as a co-purifying contaminants, when isolating HSPB5 from human, bovine and rat skeletal muscle [18,19]. Alone these two sHSPs are found as distinctly different assemblies. HSPB1 forms large oligomers, typically observed amongst representatives of this family of chaperones, while HSPB6 only forms dimers in solution [14,20–22]. Previous studies of the heterooligomers formed between recombinant HSPB1 and HSPB6 have shown that they are considerably more polydisperse in size than the component sHSPs, with a molecular weight that spans the range between the two individual proteins [21]. The heterooligomer is composed of equimolar amounts of each sHSP, a relative ratio that is fixed independent of the amount of each sHSP added to the mixture [23]. Importantly, studies using disulphide cross-linking have shown that these oligomers are principally composed of heterodimers suggesting a preferential association of HSPB1 and HSPB6 [11,23].

Currently the driving force behind the specific subunit dimerization of HSPB1 and HSPB6 is unknown. Here, we employ a variety of biophysical techniques such as size-exclusion chromatography (SEC), small-angle X-ray scattering (SAXS) and native mass spectrometry (MS) to fully characterize the biophysical properties of the HSPB1/HSPB6 heterocomplex at physiologically relevant temperatures. By using truncations, we also show that the NTDs of these proteins, regions that are typically viewed as poorly conserved and unstructured, are essential for dictating the specific association between HSPB1 and HSPB6.

2. Materials and methods

2.1 Mutagenesis and cloning

The previously described small ubiquitin modifier (SUMO) fusions of human HSPB1 and HSPB6 [24] were used as a PCR template for the generation of the two N-terminal deletion constructs. His-tagged SUMO fusion expression constructs corresponding to residues 92 to 205 of HSPB1 (HSPB1 Δ N) and residues 72 to 160 of HSPB6 (HSPB6 Δ N) were created by cloning the amplified target sequence into pETHSUL [25] using the In-Fusion® cloning kit (Clontech Laboratories). ACD constructs of both HSPB1 and HSPB6 have been reported earlier [24]. All constructs were designed such that, upon cleavage of the linearly fused SUMO chimera with recombinantly produced SUMO specific hydrolase, no additional non-native residues would be present on the target protein.

2.2 Expression and purification

Wild type HSPB1 and HSPB6, the ACD and N-terminal deletion constructs were all expressed as previously described [25,26]. Briefly, the constructs were transformed into the *E. coli* Rosetta 2 (DE3) pLysS strain and clones were cultured in ZYP-5052 auto-inducing medium [27] using described conditions [24]. Cells were harvested by centrifugation at 8000g, and resuspended in IMAC12.5 buffer (50 mM sodium phosphate, 250 mM sodium chloride and 12.5 mM imidazole, pH7.5) and stored at -80°C until further workup. For the expression of ^{15}N -labeled proteins, transformed clones were cultured in 2 mL of LB medium for 7h. This culture was then transferred to 50 mL of P0.5G-medium [27] and grown overnight at 25°C. 10 mL of this culture was spun down at 3000g and the pellet was transferred to 200 mL of auto-inducing minimal medium containing ^{15}N -ammonium chloride [27]. Cells were grown and harvested using the same protocol as the richer ZYP-5052 media.

Cells were thawed and diluted further in IMAC12.5 buffer complemented with 1

unit/mL of Cryonase Cold Active Nuclease (Clontech Laboratories) and 10 mM MgCl₂. Cells were lysed by three rounds of sonication, with a 20 min incubation period between each cycle at 4°C. Following clarification of the lysate by centrifugation at 18,000g for 1 hr at 4°C, each target fusion was purified from the supernatant by subtractive immobilized-metal affinity chromatography (IMAC), ion exchange and size exclusion chromatography (SEC) using the previously described protocols [25,26]. The ¹⁵N-labeled constructs were purified using the same procedures except the final SEC step was performed using a Superdex 200 10/300 GL column pre-equilibrated in 200 mM ammonium acetate pH 6.9 containing 2.5 mM DTT.

2.3 Formation of heterooligomeric complexes

For all analyses, recombinant HSPB1 and HSPB6 were mixed in an equimolar ratio based on their monomeric molecular weight and incubated overnight at 37°C to allow complete subunit exchange. For size-exclusion chromatography, 220 µM (corresponding to 5 mg/ml for HSPB1) of each protein was mixed in 20 mM HEPES pH 7.4, 150 mM NaCl and 10mM DTT prior to incubation.

For the native mass spectrometry experiments, 200 µM of each protein (monomer concentration) was mixed in 200 mM aqueous ammonium acetate buffer pH 6.9. All complexes were formed by overnight incubation at 37°C and were further dialyzed into the same ammonium acetate buffer containing 2.5 mM DTT to ensure complete removal of any nonvolatile salt. Samples were diluted in the same buffer to the appropriate concentration before analysis.

2.4 Analytical size-exclusion chromatography

100 µL of each protein or complex was loaded onto a Superdex 200 10/300 GL column (GE Healthcare Life Sciences), pre-equilibrated at 4°C in 20 mM HEPES pH 7.4, 150 mM NaCl and 2.5 mM DTT using a flow-rate of 0.5 mL/min. The column was calibrated using standards from the Molecular Weight Calibration kit from GE Healthcare Life Sciences. Blue dextran, ferritin, aldolase, conalbumin, ovalbumin, carbonic anhydrase, ribonuclease A and aprotinin were diluted in the same buffer and run under the same conditions.

2.5 SEC-coupled small-angle X-ray scattering

SEC-coupled small-angle X-ray scattering (SAXS) measurements were performed on the SWING beamline at Soleil Synchrotron (Gif-sur-Yvette, France) [28]. The individual sHSPs or the heterooligomeric mixture, prepared as described above, were loaded onto an

Agilent Bio SEC-3 4.6 mm by 300 mm column, with a 300 Å pore size and 3 micron bead size. The column was pre-equilibrated in 20 mM Hepes pH 7.4, 150 mM NaCl and 2.5 mM DTT and separation was performed at 0.2 ml/min. For the different temperature runs the autosampler plate, column jacket and the sample flow cell were incubated at the stated values for a minimum of 30 minutes prior to sample loading.

For each run 100 SAXS frames, measured following sample injection but preceding the column void volume, were collected for buffer subtraction. 250 sample frames were collected during the elution phase. In both cases the eluate was exposed to the X-ray beam for 1500 ms with a gap time of 500 ms between frames. Radial averaging of the collected frames, buffer averaging and subsequent subtraction from the sample data were performed using the Foxtrot application (SWING beamline). Further analysis was performed using the HPLC-SAXS module within the UltraScan Solution Modeler software package [29]. Scattering intensity profiles were generated by converting the $I(q)$ data for each frame to an $I(t)$ plot, where the measured intensity for each q -value was plotted against the frame number. From this plot the five curves for lowest q -values were scaled to the curve with the highest intensity and then averaged. For Gaussian fitting of the $I(t)$ plot a hybrid EMG+GMG function was employed. Peak positions were initially set based on their position in UV chromatogram. These values were only allowed to shift by 1% during refinement of the Gaussian function.

The molecular weight of the scattering species at a specific elution position was determined using the calculated Q_R mass parameter performed in the program ScÅtter [30]. . The $I(q)$ data corresponding to the frame at the peak maxima in the $I(t)$ plot, and the two frames either side were opened and compared to ensure similarity. These curves were then scaled together and averaged. The averaged curve was employed to calculate the R_g and volume-of-correlation (V_c), both necessary to determine Q_R .

2.6 Native mass spectrometry

All MS measurements were performed on a quadrupole/ion mobility/time-of-flight instrument (Synapt G2 HDMS, Waters, Milford, US) [31], operated in positive ion mode. Data acquisition and processing were performed using MassLynx (version 4.1) and external calibration up to 5000 m/z was performed with CsI solution. For native MS analyses, approximately 5 μ L of solution containing 20 μ M of protein (monomer concentration) in 200 mM ammonium acetate pH 6.9 containing 2.5 mM DTT was transferred to gold-coated capillaries prepared in-house and infused into the mass spectrometer using the nanoflow version of the Z-spray ion source. A capillary voltage of 1.0 – 1.3 kV and minimal (<0.2 bar)

nanoflow gas pressure were used, and the instrument was operated in Mobility/Sensitivity mode. Instrument parameters were as follows unless stated otherwise: sample cone 80 V, extraction cone 1 V, backing pressure 3.2 – 4.5 mbar, source pressure 4.6e-3 – 5.8e-3 mbar, trap collision energy 10 V, trap DC bias 50 V, transfer collision energy 5 V.

2.7 Chaperone assay

The sHSPs were assessed for their chaperoning capabilities as described previously [26]. Briefly, the substrate proteins hen egg-white lysozyme (HEWL, $M_r=14313.1$ Da), yeast alcohol dehydrogenase (yADH, monomer $M_r=36760.0$ Da) and human insulin (monomer $M_r=5795.6$ Da) were resuspended from a lyophilized powder and dialysed against 50 mM phosphate buffer pH 7.5, 100 mM NaCl. These were then incubated, in the same buffer, at a final concentration of 0.25 mg/ml with differing amounts of HSPB1, HSPB6 or an equimolar mix of the two sHSPs. The calculated substrate:sHSP ratio was based on the monomer molecular weight of each substrate, HSPB1 ($M_r=22782.5$ Da) and HSPB6 ($M_r=17135.6$ Da), or the average molecular weight of HSPB1 and HSPB6 combined for the heterooligomeric mix. Aggregation of insulin and HEWL was induced by the addition of 10 mM DTT at 37°C. For yADH 20 mM DTT and 2 mM EDTA was added and the mixture incubated at 42°C. Chaperone activity was monitored by measuring the absorbance at 340 nm.

3. Results

3.1 Activity of recombinantly produced sHSPs

It was previously reported that HSPB1 and HSPB6, when mixed in an equimolar fashion, form a broad polydisperse population. These earlier experiments were carried out using recombinant protein that was purified by ammonium sulfate fractionation followed by anion exchange chromatography and hydrophobic interaction or SEC [21,23]. As we isolated the protein using the SUMO fusion technology, it was initially investigated whether these results could be replicated. Analysis of the heterooligomeric complex by analytical SEC at 4°C showed a polydisperse mixture containing two main peaks around 508 and 166 kDa (Fig. 1A). SDS-PAGE analysis of the eluted fractions showed a 1:1 ratio of both sHSPs across the whole chromatogram (Fig. 1B), in line with earlier data [23].

In addition to examining the solution properties, the chaperone activity of the heterooligomeric species formed between recombinant HSPB1 and HSPB6 was also assessed. Using reduced insulin as a substrate the heterooligomer showed an increased capacity to prevent aggregation when compared to the component sHSPs alone at all ratios tested (Fig. 1C and Supplemental Fig. 1). With γ ADH the sHSP mixture demonstrated a small enhancement in chaperone-like activity that was most significant at the 10:1 ratio between γ ADH and the two sHSPs combined (Fig. 1D and Supplemental Fig. 1). Finally, using HEWL as a substrate, the heterooligomer demonstrated activity that was intermediate of HSPB1 and HSPB6 alone (Fig. 1E and Supplemental Fig. 1). Notably, as previously reported, HSPB6 appears to co-aggregate with denatured lysozyme [26]. By pre-mixing HSPB1 and HSPB6 together this is prevented, but it results in a mild reduction in chaperone-like activity relative to HSPB1 alone for all substrate:sHSP concentration ratios tested.

3.2 SEC-coupled SAXS characterization

To obtain a better understanding of the biophysical properties of the different heterooligomeric species observed in analytical SEC a similarly prepared sample was also examined by SEC-coupled SAXS. In this case the heterooligomer was also examined by loading equivalent sample volumes, of the same pre-incubated mixture, diluted to different concentrations onto the column (Fig. 2A). As before a UV-chromatogram composed of two overlapping peaks was observed but, at lower concentrations, the ratio of the two peaks changed, with the lower molecular weight species becoming more dominant. Examination of the plots of scattering intensity versus elution time shows a similar result, albeit the larger,

earlier eluting species dominates the profile resulting in lower resolution between the two species (Fig. 2B). For all three loaded concentrations the calculated radius of gyration (R_g) across the whole SAXS elution profile are similar. This suggests that while the distribution of the different species depends on the protein concentration, the sizes of the component entities remain equivalent. Taking this into account, the SAXS data from the middle concentration was decomposed using two skewed Gaussians (Fig. 2C). Using the SAXS curves from the maxima of the decomposed Gaussian peaks a molecular weight of 306.9 and 95.2 kDa was determined based on the calculated Q_R parameter [30]. These values are equivalent to heterooligomeric assemblies with an average number of subunits of 15 and 4, respectively.

As the above experiments were performed at 15°C, we also investigated the effect of temperature on the relative distribution of the heterooligomeric assemblies formed between HSPB1 and HSPB6 using SEC-coupled SAXS (Fig. 3). For comparison the two sHSPs were also individually run under the same conditions. For HSPB1 and HSPB6 alone, raising the temperature to a physiologically relevant value had an opposite effect. In the case of HSPB1 the protein eluted earlier from the Bio SEC-3 column, while HSPB6 showed a 2.5 minute delay in exiting the column upon raising the temperature from 15°C to 37°C (Fig. 3A). Analysis of the SAXS data showed that, in the case of HSPB1, the reduction in the elution volume correlated well with an increase in the size of the oligomer as determined from the R_g and the molecular weight (Fig. 3B, Supplemental Fig. 2 and Table 1). Specifically the observed change in mass resulted in the recruitment of four additional subunits at 37°C, when compared to the lower temperature experiments. In the case of HSPB6, despite the dramatic increase in the elution volume, the R_g and calculated molecular weight was similar for all experiments (Fig. 3B and Table 1). The measured values are consistent with it preferentially being a dimer in solution, as has been previously reported [20,21]. This suggests that at elevated temperatures HSPB6 non-specifically associates with the column resin. As this effect is temperature-dependent it is likely the result of an increase in HSPB6 hydrophobicity.

At all measured temperatures, the preheated equimolar mixture of HSPB1 and HSPB6 showed a clear polydisperse ensemble (Fig. 3A). In comparison to the two sHSPs alone, the elution position and absorbance of the maxima of the larger heterooligomeric species remained relatively constant, showing that temperature had a smaller effect on the size of this entity. This was further confirmed by analysis of the SAXS curves at the peak maxima, which suggest the addition of only two subunits over the measured temperature range (Table 1). For the smaller tetrameric species, observed as a clear peak at 4 and 15°C, raising the temperature to physiological values resulted in a less resolved profile (Figs. 2A and 3A). The relative

height of this peak to the larger species reduces, whilst at the same time the overall profile becomes more asymmetric showing distinct tailing that extends to later elution volumes (Fig. 3A and B). This behavior partially mirrors that of HSPB6 alone, suggesting that the smaller heterocomplex also becomes more hydrophobic at elevated temperatures resulting in an increase in non-specific interaction with the column matrix. Despite the extended elution profile comparison of the calculated R_g across the heterooligomer peak were similar at the different temperatures (Figs. 2C and 3B). Importantly, even at the lowest determined values, the R_g of the heterooligomer was always greater than that calculated for the dimeric HSPB6 (Fig. 3B). This suggests that under the studied conditions the complex does not dissociate to this smaller building block but rather remains as a tetramer in its smallest form.

3.3 Native MS analysis shows that HSPB1 and HSPB6 form heterodimers in a preferential manner

We additionally analyzed the heterocomplex between HSPB1 and HSPB6 using native MS (Fig. 4). This technique provides an accurate measurement of the molecular mass of the species present in the gas phase, and permits analysis of the size and stoichiometry of the component entities. Annotation of the spectra showed the prevalence of heterodimeric and heterotetrameric populations with a low abundance of higher molecular weight oligomers (Fig. 4A). At the 20 μM (0.4 mg/ml) employed the species distribution extends the analysis of the effect of protein concentration on oligomer size, initially performed with SAXS-coupled SEC (Fig. 2A), showing also a predisposition of the heterooligomer to dissociate into small entities at lower concentrations.

Importantly, careful examination of the MS spectrum of the heterooligomeric mixture showed no peaks corresponding to a homodimer of HSPB6 or HSPB1, nor peaks corresponding to the larger HSPB1 oligomeric species (Fig. 4A-C). This suggests that complete exchange of the individual subunits has occurred forming entities built from a HSPB1 and HSPB6 heterodimer. This specific heterodimerisation is surprising, as random exchange of the individual protomers would be predicted to lead to oligomers containing a mixture of heterodimers and homodimers at equilibrium. Such stochastic exchange was observed by native MS analysis of HSPB1 and HSPB6 alone, using mixtures of equimolar amounts of ^{15}N -labeled and unlabeled protein (Figs. 4D and E). Following incubation, under the same conditions used for heterooligomer formation, the MS spectra of each sHSP showed a 1:2:1 ratio of unlabeled homodimer, heterodimer (^{15}N -labeled and unlabeled), and ^{15}N -labeled homodimer, respectively. Taken together these results demonstrate that when mixed

HSPB1 and HSPB6 have a clear preference to form species composed of heterodimers.

3.4 The N-terminal domain is required for preferential heterooligomerization

To delineate the necessary regions for this preferential heterodimerization, both HSPB1 and HSPB6 were truncated to either the α -crystallin domain (ACD) alone or the ACD containing the C-terminal domain (CTD), termed ΔN (Fig. 5). Native MS analysis showed that all four constructs alone had the capacity to dimerize (Supplemental Fig. S3). The truncations were therefore analyzed for their capacity to form a heterodimeric complex by this high resolution method. For both truncations, heterodimeric species were observed together with homo-dimers in an approximate 1:2:1 ratio (Fig. 6A and B, inserts). Although deletion of the N-terminal domains (NTDs) does not appear to limit subunit exchange, their removal results in a purely stochastic association of the component protomers (Fig. 6).

Under the conditions used, monomeric species were also observed in the mass spectra for all truncations, suggesting that the NTD-trimmed dimers are less stably associated than the full-length proteins. Gas-phase stability assays of the construct mixtures, where the trap collision energy was increased by 10 V increments, were performed to assess the relative strength of the different dimer interfaces in the gas phase (Fig. 6C and D, Supplemental Fig. 4). The relative strength of the ACD dimer interface is highly similar for HSPB6, HSPB1 and the heterodimer (Fig. 6C). For the ΔN constructs, the presence of the CTD resulted in a modest increase in the heterodimer interface strength when compared to the two homodimer interfaces (Fig. 6D).

Taken together, both the stochastic exchange of subunits and the similar stability of the heterodimer interface, show that neither the structured ACD nor the C-terminal regions of the two sHSPs have a profound role in the preferential association of full-length HSPB1 and HSPB6. The CTD seems to have a mildly stabilizing effect, although it does not seem to influence the association of both constructs as the ratio of homo vs. heterodimer was still approximately 1:2:1. The determinant region of this heterodimeric association is thus the absent NTD, a sequence that is predicted to be predominantly unstructured.

4. Discussion

Heterooligomerization between sHSP orthologues has long been recognized in different organisms. Class-specific homologues isolated from some bacteria or plants have been demonstrated to associate with each other *in vitro* [7,8,32]. In vertebrates considerably more evidence supports the existence of heterooligomers *in vivo*. Classically this includes the α -crystallins of the eye lens, but numerous other vertebrate sHSPs have been indicated as co-assembling [6,11]. Typically the interaction between two or more sHSPs appears to be stochastic in nature, where the representation of each component in the mixed oligomer purely reflects their input concentration [14,22]. However, a number of vertebrate sHSPs have been shown to form heterooligomers that contain a fixed ratio of the component protomers, independent of the starting proportions used [16,23]. The molecular determinants that define such specificity are poorly understood.

We have characterized the heterooligomers formed between human HSPB1 and HSPB6, two sHSPs that are highly expressed in muscle tissue [17]. Together both proteins form highly polydisperse assemblies where the predominant species have masses centered at 283.2 and 76.4 kDa. This profile, as shown previously [23], can be altered by varying the concentration of the sHSP mixture, where lower concentrations favor the smaller assembly (Fig. 2). This behavior appears to be a combination of the solution properties of the component sHSPs. HSPB1 forms large oligomers comprised of close to 30 monomers, whereas HSPB6 is predominantly found as a dimer in solution (Table 1). The two major species seen for the HSPB1-HSPB6 heterooligomers are both considerably smaller than the HSPB1 oligomers, likely an influence of HSPB6. At the same time the smaller heterooligomeric entity is principally a tetramer, even at low concentrations, pointing to the influence of HSPB1 on assembly. SEC-coupled SAXS analysis of the effect of temperature on the species distribution of the heterooligomer showed that raising the sample to physiological temperatures resulted in no increase in disassembly of the larger entity. Interestingly the tetrameric species demonstrated a non-specific association with the column matrix, similar to that of HSPB6 alone, alluding to an increase in hydrophobicity of the parent sHSP and its influence on the properties of the smaller heterooligomeric species (Fig. 3).

The readiness to form smaller assemblies, typically recognized as the active state in this family of chaperones [3,4,8], suggest that the HSPB1/HSPB6 heterooligomer may have a higher propensity to protect denaturing proteins. Using HEWL, which HSPB6 alone completely fails to chaperone, the heterooligomer demonstrated a capacity to prevent

aggregation although not as effectively as HSPB1 (Fig. 1D). With yADH, at higher substrate:sHSP ratios, a small increase in activity over the individual sHSPs was observed, while with insulin the activity of the heterooligomer was significantly greater than the parent sHSPs (Figs. 1C and D). Combined these results show, in the worst case, that the heterooligomer has a capacity to chaperone that is equal to the average of the percentage protection afforded by HSPB1 and HSPB6 alone. Ultimately though, it does hint at a possible enhancement in overall chaperone activity. The observed range of protection is likely a limitation of the substrates tested. Future experiments should include an evaluation of more biologically relevant proteins, as well as analyzing whether there are differences in substrate specificity between the individual sHSPs and their amalgam.

In order to delineate the sequence determinants that dictate heterooligomer formation between these two sHSPs, we have employed nanoelectrospray mass spectrometry. Using conditions that maintained the native state, analysis of the heterooligomer clearly showed the presence of a heterodimer as the core building block of the larger assemblies (Fig. 4). This result is in excellent agreement with disulphide cross-linking experiments that employed a double mutant of HSPB6 and the wild-type HSPB1 [11,23]. Crucially in the present study, using the wild-type sequence for both proteins, we did not observe any peaks corresponding to the homo-dimers of HSPB1 or HSPB6, or higher order assemblies of the former. Thus under the conditions employed subunit exchange was complete and biased to heterodimeric association. This behavior is different to the two sHSPs alone that demonstrated simple stochastic exchange at the monomer level, as observed by the free exchange of heavy and light subunits (Fig. 4D an E).

Structurally a sHSP chain consists of an N-terminal domain (NTD), the central α -crystallin domain (ACD) and the C-terminal domain (CTD). The ACD has a β -sandwich fold and is responsible for dimer formation, while the NTD and CTD are predicted to be disordered [20,33]. Limited proteolysis and X-ray crystallographic studies of vertebrate sHSPs, point to ACD as being the sole temporally stable structured region in these proteins [20,24,34]. This domain, and in particular the β 7-strand, forms the principal dimer interface between protomers in the higher order assemblies [20,34,35]. It is therefore logical to hypothesize that the ACD, and the specific sequence differences in this region between HSPB1 and HSPB6, dictate the preferential heterodimerization observed when mixing together the two full-length proteins. Surprisingly though the isolated ACDs demonstrated stochastic exchange with each other (Fig. 6). Additional gas-phase stability experiments also showed that the strength of the ACD dimer interface was similar for both the parent homo-

dimers and the heterodimer. Therefore the ACD, although important as the dimerization interface, has no role in the preferred association of HSPB1 and HSPB6.

Previous studies have demonstrated that the IXI/V motif contained in the CTD can influence the strength of the ACD dimer [36]. Specifically, substitution of the residues 159-161 of human α B-crystallin with alanines reduced binding of the CTD to the β 4/ β 8 face of the ACD and resulted in stabilization of the β 7-mediated dimer interface. As HSPB6 does not contain the canonical C-terminal IXI/V motif (Fig. 5) it could be rationalized that the mixing of this sHSP with HSPB1 would lead to a more stable heterodimer interface, which is indeed observed with the Δ N deletion constructs (Fig. 6C and D). Despite this apparent increase in the stability of the ACD heterodimer, at equilibrium the overall distribution of the individual truncated protomers between homo and heterodimer is still stochastic suggesting that the CTD has little to no influence on the preferred association of HSPB1 and HSPB6.

The various sHSP truncations ultimately point to the NTD, a region predicted to be unstructured [20,33], as being essential for driving the specific heterodimerization of HSPB1 and HSPB6. The involvement of the NTD in defining the heterodimer interface, located at the ACD, is quite remarkable. Truncation or post-translational modification of this region often leads to smaller assemblies typically pointing to its recognized role in higher-order oligomerization rather than dimer formation [33]. It was reported that phosphorylation of the N-terminal serine residues of HSPB5 led to a loss of the dimeric substructure within the larger oligomer species, but this was hypothesized to be the result of a reduced interaction of individual subunits within the whole assembly [37].

In the present study, the NTDs appear to have a role in stabilizing the smaller heterodimer containing species, most clearly seen by the absence of monomers in the native MS analysis of the full-length heterodimeric protein compared to the two truncations under identical conditions (Figs. 4 and 5). This suggests the possibility of cross-talk between one or both of the NTDs and the heterodimer ACD, via a molecular mechanism that is absent in the homo-oligomeric species. Future experiments should attempt to discern the specific sequence epitopes that define this interaction, which appears non-trivial due to poor sequence conservation in the majority of the NTD [26,33].

Conflict of interest statement

The authors declare that there is no conflict of interest in this work.

Acknowledgements

This research was supported by the Research Foundation Flanders (FWO) grants G093615N and WO03315N as well as by the KU Leuven grant OT13/097 (all to S.V.S.). M.H. has held a teaching assistant grant from the Department of Pharmaceutical and Pharmacological Sciences, KU Leuven. We also thank the FWO for funding a PhD fellowship of F.L. (grant no. 11L4115N) and the Hercules Foundation Flanders for funding the Synapt instrument. We acknowledge support from the European Community's Seventh Framework Programme under the BioStruct-X initiative (project number 6131) towards the synchrotron SAXS measurements. The authors further greatly appreciate the excellent support from the beamline scientists on the SWING beamline (Soleil Synchrotron, France).

References

- [1] E. Basha, H. O'Neill, E. Vierling, Small heat shock proteins and α -crystallins: dynamic proteins with flexible functions, *Trends Biochem. Sci.* 37 (2012) 106–117. doi:10.1016/j.tibs.2011.11.005.
- [2] T.M. Treweek, S. Meehan, H. Ecroyd, J.A. Carver, Small heat-shock proteins: important players in regulating cellular proteostasis, *Cell. Mol. Life Sci. CMLS*. 72 (2015) 429–451. doi:10.1007/s00018-014-1754-5.
- [3] H.S. Mchaourab, J.A. Godar, P.L. Stewart, Structure and mechanism of protein stability sensors: chaperone activity of small heat shock proteins, *Biochemistry (Mosc.)*. 48 (2009) 3828–3837. doi:10.1021/bi900212j.
- [4] M. Haslbeck, E. Vierling, A First Line of Stress Defense: Small Heat Shock Proteins and Their Function in Protein Homeostasis, *J. Mol. Biol.* 427 (2015) 1537–1548. doi:<http://dx.doi.org/10.1016/j.jmb.2015.02.002>.
- [5] G.K.A. Hochberg, J.L.P. Benesch, Dynamical structure of α B-crystallin, *Prog. Biophys. Mol. Biol.* 115 (2014) 11–20. doi:10.1016/j.pbiomolbio.2014.03.003.
- [6] A.-P. Arrigo, Human small heat shock proteins: Protein interactomes of homo- and heterooligomeric complexes: An update, *FEBS Lett.* 587 (2013) 1959–1969. doi:10.1016/j.febslet.2013.05.011.
- [7] S. Studer, F. Narberhaus, Chaperone activity and homo- and heterooligomer formation of bacterial small heat shock proteins, *J. Biol. Chem.* 275 (2000) 37212–37218. doi:10.1074/jbc.M004701200.
- [8] E. Basha, C. Jones, V. Wysocki, E. Vierling, Mechanistic differences between two conserved classes of small heat shock proteins found in the plant cytosol, *J. Biol. Chem.* 285 (2010) 11489–11497. doi:10.1074/jbc.M109.074088.
- [9] G. Kappé, E. Franck, P. Verschuur, W.C. Boelens, J.A.M. Leunissen, W.W. de Jong, The human genome encodes 10 alpha-crystallin-related small heat shock proteins: HspB1-10, *Cell Stress Chaperones*. 8 (2003) 53–61.
- [10] J.-M. Fontaine, X. Sun, R. Benndorf, M.J. Welsh, Interactions of HSP22 (HSPB8) with HSP20, alphaB-crystallin, and HSPB3, *Biochem. Biophys. Res. Commun.* 337 (2005) 1006–1011. doi:10.1016/j.bbrc.2005.09.148.
- [11] E.V. Mymrikov, A.S. Seit-Nebi, N.B. Gusev, Heterooligomeric complexes of human small heat shock proteins, *Cell Stress Chaperones*. 17 (2012) 157–169. doi:10.1007/s12192-011-0296-0.
- [12] A. Spector, L.K. Li, R.C. Augusteyn, A. Schneider, T. Freund, -Crystallin. The isolation and characterization of distinct macromolecular fractions, *Biochem. J.* 124 (1971) 337–343.
- [13] R.C. Augusteyn, alpha-crystallin: a review of its structure and function, *Clin. Exp. Optom. J. Aust. Optom. Assoc.* 87 (2004) 356–366.
- [14] F. Skouri-Panet, M. Michiel, C. Férand, E. Duprat, S. Finet, Structural and functional specificity of small heat shock protein HspB1 and HspB4, two cellular partners of HspB5: role of the in vitro heterocomplex formation in chaperone activity, *Biochimie*. 94 (2012) 975–984. doi:10.1016/j.biochi.2011.12.018.
- [15] J.A. Thomson, R.C. Augusteyn, On the structure of alpha-crystallin: construction of hybrid molecules and homopolymers, *Biochim. Biophys. Acta*. 994 (1989) 246–252.
- [16] J. den Engelsman, S. Boros, P.Y.W. Dankers, B. Kamps, W.T. Vree Egberts, C.S. Böde, L.A. Lane, J.A. Aquilina, J.L.P. Benesch, C.V. Robinson, W.W. de Jong, W.C. Boelens, The small heat-shock proteins HSPB2 and HSPB3 form well-defined heterooligomers in a unique 3 to 1 subunit ratio, *J. Mol. Biol.* 393 (2009) 1022–1032. doi:10.1016/j.jmb.2009.08.052.

- [17] M.J. Vos, B. Kanon, H.H. Kampinga, HSPB7 is a SC35 speckle resident small heat shock protein, *Biochim. Biophys. Acta.* 1793 (2009) 1343–1353. doi:10.1016/j.bbamcr.2009.05.005.
- [18] K. Kato, S. Goto, Y. Inaguma, K. Hasegawa, R. Morishita, T. Asano, Purification and characterization of a 20-kDa protein that is highly homologous to alpha B crystallin, *J. Biol. Chem.* 269 (1994) 15302–15309.
- [19] K. Kato, H. Shinohara, S. Goto, Y. Inaguma, R. Morishita, T. Asano, Copurification of small heat shock protein with alpha B crystallin from human skeletal muscle, *J. Biol. Chem.* 267 (1992) 7718–7725.
- [20] S.D. Weeks, E.V. Baranova, M. Heirbaut, S. Beelen, A.V. Shkumatov, N.B. Gusev, S.V. Strelkov, Molecular structure and dynamics of the dimeric human small heat shock protein HSPB6, *J. Struct. Biol.* 185 (2014) 342–354. doi:10.1016/j.jsb.2013.12.009.
- [21] O.V. Bukach, A.S. Seit-Nebi, S.B. Marston, N.B. Gusev, Some properties of human small heat shock protein Hsp20 (HspB6), *Eur. J. Biochem.* 271 (2004) 291–302. doi:10.1046/j.1432-1033.2003.03928.x.
- [22] J.A. Aquilina, S. Shrestha, A.M. Morris, H. Ecroyd, Structural and functional aspects of heterooligomers formed by the small heat shock proteins α B-crystallin and HSP27, *J. Biol. Chem.* 288 (2013) 13602–13609. doi:10.1074/jbc.M112.443812.
- [23] O.V. Bukach, A.E. Glukhova, A.S. Seit-Nebi, N.B. Gusev, Heterooligomeric complexes formed by human small heat shock proteins HspB1 (Hsp27) and HspB6 (Hsp20), *Biochim. Biophys. Acta BBA - Proteins Proteomics.* 1794 (2009) 486–495. doi:10.1016/j.bbapap.2008.11.010.
- [24] E.V. Baranova, S.D. Weeks, S. Beelen, O.V. Bukach, N.B. Gusev, S.V. Strelkov, Three-Dimensional Structure of α -Crystallin Domain Dimers of Two Human Small Heat Shock Proteins, HSPB1 and HSPB6, *J. Mol. Biol.* 411 (2011) 110–122. doi:10.1016/j.jmb.2011.05.024.
- [25] S.D. Weeks, M. Drinker, P.J. Loll, Ligation independent cloning vectors for expression of SUMO fusions, *Protein Expr. Purif.* 53 (2007) 40–50. doi:10.1016/j.pep.2006.12.006.
- [26] M. Heirbaut, S. Beelen, S.V. Strelkov, S.D. Weeks, Dissecting the Functional Role of the N-Terminal Domain of the Human Small Heat Shock Protein HSPB6, *PloS One.* 9 (2014) e105892. doi:10.1371/journal.pone.0105892.
- [27] F.W. Studier, Protein production by auto-induction in high density shaking cultures, *Protein Expr. Purif.* 41 (2005) 207–234.
- [28] G. David, J. Pérez, Combined sampler robot and high-performance liquid chromatography: a fully automated system for biological small-angle X-ray scattering experiments at the Synchrotron SOLEIL SWING beamline, *J. Appl. Crystallogr.* 42 (2009) 892–900. doi:10.1107/S0021889809029288.
- [29] E. Brookes, J. Pérez, B. Cardinali, A. Profumo, P. Vachette, M. Rocco, Fibrinogen species as resolved by HPLC-SAXS data processing within the UltraScan Solution Modeler (US-SOMO) enhanced SAS module, *J. Appl. Crystallogr.* 46 (2013) 1823–1833. doi:10.1107/S0021889813027751.
- [30] R.P. Rambo, J.A. Tainer, Accurate assessment of mass, models and resolution by small-angle scattering, *Nature.* 496 (2013) 477–481. doi:10.1038/nature12070.
- [31] S.D. Pringle, K. Giles, J.L. Wildgoose, J.P. Williams, S.E. Slade, K. Thalassinos, R.H. Bateman, M.T. Bowers, J.H. Scrivens, An investigation of the mobility separation of some peptide and protein ions using a new hybrid quadrupole/travelling wave IMS/o-ToF instrument, *Int. J. Mass Spectrom.* 261 (2007) 1–12. doi:10.1016/j.ijms.2006.07.021.
- [32] F. Sobott, J.L.P. Benesch, E. Vierling, C.V. Robinson, Subunit exchange of multimeric protein complexes. Real-time monitoring of subunit exchange between small heat shock

- proteins by using electrospray mass spectrometry, *J. Biol. Chem.* 277 (2002) 38921–38929. doi:10.1074/jbc.M206060200.
- [33] M. Heirbaut, S.V. Strelkov, S.D. Weeks, Everything but the ACD, Functional Conservation of the Non-conserved Terminal Regions in sHSPs, in: R.M. Tanguay, L.E. Hightower (Eds.), *Big Book Small Heat Shock Proteins*, Springer International Publishing, 2015: pp. 197–227. doi:10.1007/978-3-319-16077-1_8.
- [34] C. Bagnérés, O.A. Bateman, C.E. Naylor, N. Cronin, W.C. Boelens, N.H. Keep, C. Slingsby, Crystal structures of alpha-crystallin domain dimers of alphaB-crystallin and Hsp20, *J. Mol. Biol.* 392 (2009) 1242–1252. doi:10.1016/j.jmb.2009.07.069.
- [35] G.K.A. Hochberg, H. Ecroyd, C. Liu, D. Cox, D. Cascio, M.R. Sawaya, M.P. Collier, J. Stroud, J.A. Carver, A.J. Baldwin, C.V. Robinson, D.S. Eisenberg, J.L.P. Benesch, A. Laganowsky, The structured core domain of α B-crystallin can prevent amyloid fibrillation and associated toxicity, *Proc. Natl. Acad. Sci. U. S. A.* 111 (2014) E1562–1570. doi:10.1073/pnas.1322673111.
- [36] G.R. Hilton, G.K.A. Hochberg, A. Laganowsky, S.I. McGinnigle, A.J. Baldwin, J.L.P. Benesch, C-terminal interactions mediate the quaternary dynamics of α B-crystallin, *Philos. Trans. R. Soc. Lond. B. Biol. Sci.* 368 (2013) 20110405. doi:10.1098/rstb.2011.0405.
- [37] J.A. Aquilina, J.L.P. Benesch, L.L. Ding, O. Yaron, J. Horwitz, C.V. Robinson, Phosphorylation of B-Crystallin Alters Chaperone Function through Loss of Dimeric Substructure, *J. Biol. Chem.* 279 (2004) 28675–28680. doi:10.1074/jbc.M403348200.
- [38] L. Seleno, D.A. Volmer, Ion activation methods for tandem mass spectrometry, *J. Mass Spectrom. JMS.* 39 (2004) 1091–1112. doi:10.1002/jms.703.
- [39] L. Han, S.-J. Hyung, J.J.S. Mayers, B.T. Ruotolo, Bound anions differentially stabilize multiprotein complexes in the absence of bulk solvent, *J. Am. Chem. Soc.* 133 (2011) 11358–11367. doi:10.1021/ja203527a.
- [40] L. Han, S.-J. Hyung, B.T. Ruotolo, Bound cations significantly stabilize the structure of multiprotein complexes in the gas phase, *Angew. Chem. Int. Ed Engl.* 51 (2012) 5692–5695. doi:10.1002/anie.201109127.

Figure legends

Fig. 1. Characterization of the HSPB1-HSPB6 heterooligomer. (A) Analytical gel-filtration profile of an equimolar mixture of HSPB1 and HSPB6 loaded directly onto the column after mixing at 4°C (black curve), or following overnight incubation at 37°C (grey dashed curve). A 100 μ l sample was loaded onto a Superdex 200 10/300 column equilibrated in 20 mM HEPES, 150 mM NaCl and 2.5 mM DTT. Eluted fraction positions are labeled above the abscissa. (B) SDS-PAGE analysis of the fractions from analytical gel-filtration. Fraction numbers above the gel correspond to panel A. An input sample (i) of the equimolar mix of both sHSPs taken prior to injection onto the column, and the same sample diluted 10-fold (i/10) were also loaded. (C-E) Chaperone activity of the heterooligomeric complex compared to B1 and B6 alone. Aggregation was monitored by following the absorbance at 340 nm for 90 min. The percentage of protection for each construct was calculated as described in Materials and Methods. (C) 0.25 mg/ml insulin incubated with HSPB1 or HSPB6 alone or the HSPB1-HSPB6 complex. Aggregation was induced by addition of 10 mM DTT (final concentration) prior to continuous measurement at 37°C. The ratios of substrate to sHSP are 1:0.2 (black bars), 1:0.1 (gray bars) and 1:0.05 (light gray bars). (D) 0.25 mg/ml γ ADH as substrate. Aggregation was induced by the addition of 20 mM DTT and 2 mM EDTA (final concentrations) prior to measurement at 42°C. The ratios used are 1:2 (black bars), 1:1 (gray bars) and 1:0.5 (light gray bars). (E) Time dependent aggregation of HEWL. Following preincubation at 37°C aggregation was induced by addition of 10 mM DTT (final concentration). 0.25 mg/ml of HEWL was used as a substrate in a 1:2 monomer molar ratio with the specified sHSP.

Fig. 2. SEC-coupled SAXS analysis of the HSPB1-HSPB6 heterooligomer (A) UV based chromatogram showing the effect of the loaded sample concentration on the species distribution of an equimolar mixture of HSPB1 and HSPB6. The mixed sHSPs were pre-incubated overnight at 37°C. The highest concentration sample was then appropriately diluted in 20 mM Hepes pH 7.4, 150 mM NaCl and 2.5 mM DTT. 25 μ l of each sample was loaded onto an analytical Agilent Bio SEC-3 column pre-equilibrated in the same buffer. The column temperature was maintained at 15°C. (B) The corresponding SAXS intensity profiles (lines) normalized by the maxima (C_{\max}) of the UV-chromatogram (see the Methods for a full definition of the value plotted). The calculated radius of gyration (R_g) across the eluting peak for each concentration is represented as dots. For clarity only every other point is plotted. 217.5 μ g (red line and dots), 108.8 μ g (black lines and dots), 54.5 μ g (blue lines and dots). (C) Gaussian decomposition of the intensity profile of the 108.8 μ g loaded sample. The measured intensities and calculated R_g across the whole peak are shown in black lines and dots, respectively. The two skewed Gaussian fits (blue and cyan) and their sum (red) are shown overlaying the intensity data. The corresponding calculated R_g across the decomposed peaks are shown in the same colours.

Fig. 3. Effect of temperature on HSPB1 and HSPB6 and their heterooligomeric complexes (A) Overlaid UV chromatograms of SEC runs of HSPB1 and HSPB6 alone and their equimolar mixture at various temperatures. The mixed sHSPs were pre-incubated overnight at 37°C. 25 μ l of each sample was loaded onto an analytical Agilent Bio SEC-3 column pre-equilibrated in 20 mM Hepes pH 7.4, 150 mM NaCl and 2.5 mM DTT. Both the autosampler and the column were pre-incubated at the stated temperatures for 30 minutes before application of the sample. The vertical dashed lines correspond to the maxima position for HSPB1 and HSPB6 at 15°C. (B) Overlaid SAXS intensity profiles of HSPB1 at 15°C (dashed red line) and 30°C (red line), HSPB6 at 15°C (dashed blue line) and 30°C (blue line), and the

heterooligomeric mix at 30°C (black line). The corresponding Rg for each peak are shown as empty (15°C) or filled (30°C) circles in the same colour as the respective intensity plot.

Fig. 4. Native mass spectrometry analysis of HSPB1, HSPB6 and their heterooligomeric complexes. Annotated spectra from native MS of the HSPB1-HSPB6 heterocomplex (A), HSPB1 (B) and HSPB6 (C). For each sample an equivalent of 20 μ M monomer concentration of protein, diluted in 200 mM ammonium acetate pH 6.9 containing 2.5 mM DTT, was analyzed on a Synapt G2 HDMS (Waters). Charge states and the species identity are indicated above each peak. The number of circles above the annotated peaks corresponds to the oligomeric state of the identified species. (D) A zoom in of the 13+ charge state from the native MS profile of HSPB1 that had been pre-mixed with equimolar amounts of ^{15}N -labeled HSPB1. (E) A zoom of the 11+ charge state from the native MS profile of HSPB6 pre-mixed with equimolar amounts of ^{15}N -labeled HSPB6.

Fig. 5. HSPB1 and HSPB6 deletion constructs. The different sHSP truncations, and their residue ranges, are shown relative to the corresponding full-length protein. Domain boundaries for the ACD are based on X-ray crystal structures [33]. The NTD and CTD for both constructs are shaded in gray. The sequence and position of the highly conserved C-terminal IXI/V motif is shown for HSPB1.

Fig. 6. Native mass spectrometry analysis of truncated HSPB1 and HSPB6 constructs. (A) Native MS of the heterooligomeric mixture of HSPB1.ACD and HSPB6.ACD in a 1:1 ratio. (B) Native MS of the heterooligomeric mixture of HSPB1. ΔN and HSPB6. ΔN in a 1:1 ratio. (C) Graph showing the results of the gas-phase stability assay where the trap collision energy was increased with 10 V increments on the sample containing the equimolar mixture of HSPB1.ACD and HSPB6.ACD (orange line), HSPB1.ACD alone (red line) and HSPB6.ACD alone (green line). (D) Graph showing the results of the gas-phase stability assay where the trap collision energy was increased with 10 V increments on the sample containing the equimolar mixture of HSPB1. ΔN and HSPB6. ΔN (orange line), HSPB1. ΔN (red line) alone and HSPB6. ΔN alone (green line). Inserts in panels (A) and (B) show relative abundances of the different homo- and heterodimers as determined after spectral deconvolution. Normalized collision energies in panels (C) and (D) were calculated according to standard procedures [38–40]. Dotted lines in (C) and (D) indicate the energy required to obtain 50% dissociation yield.

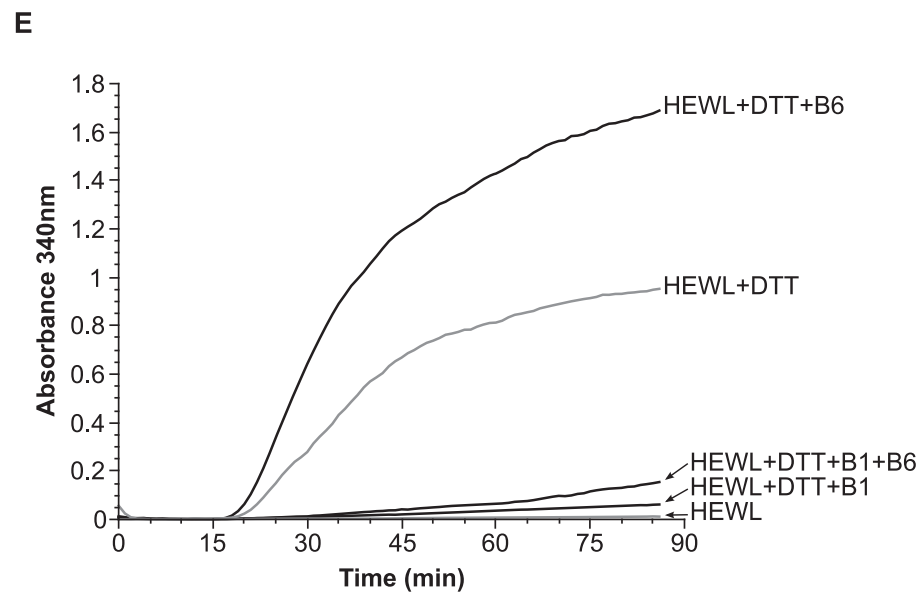
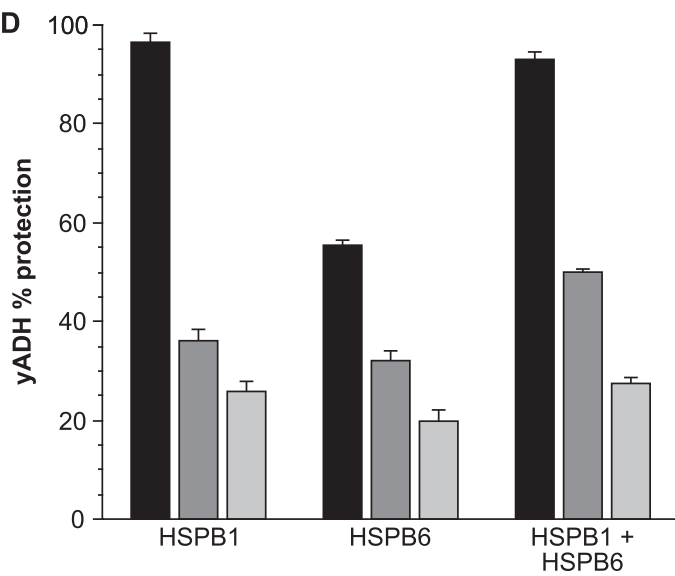
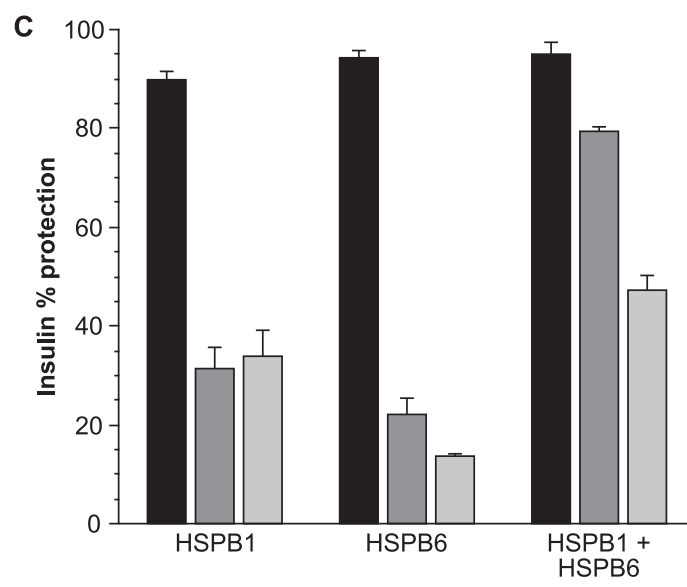
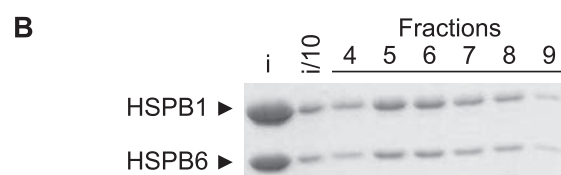
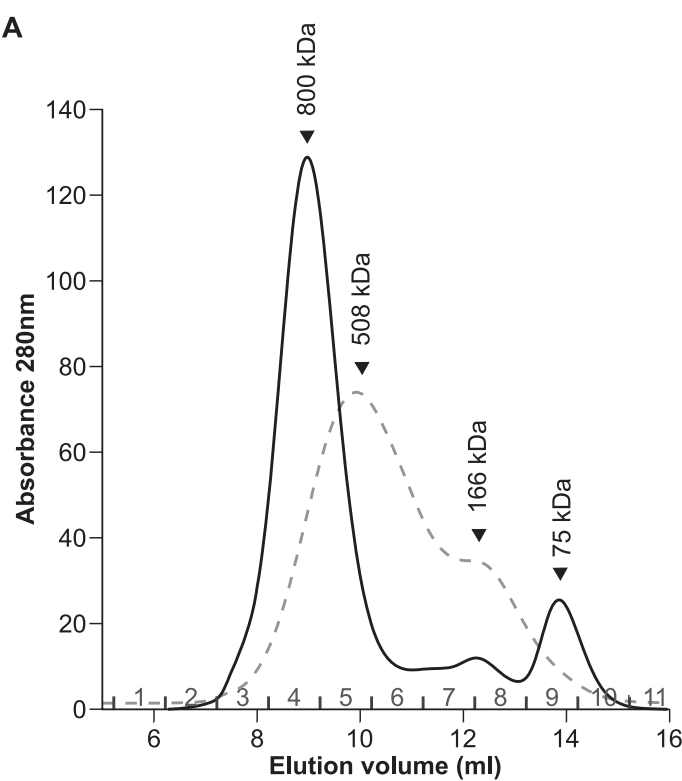
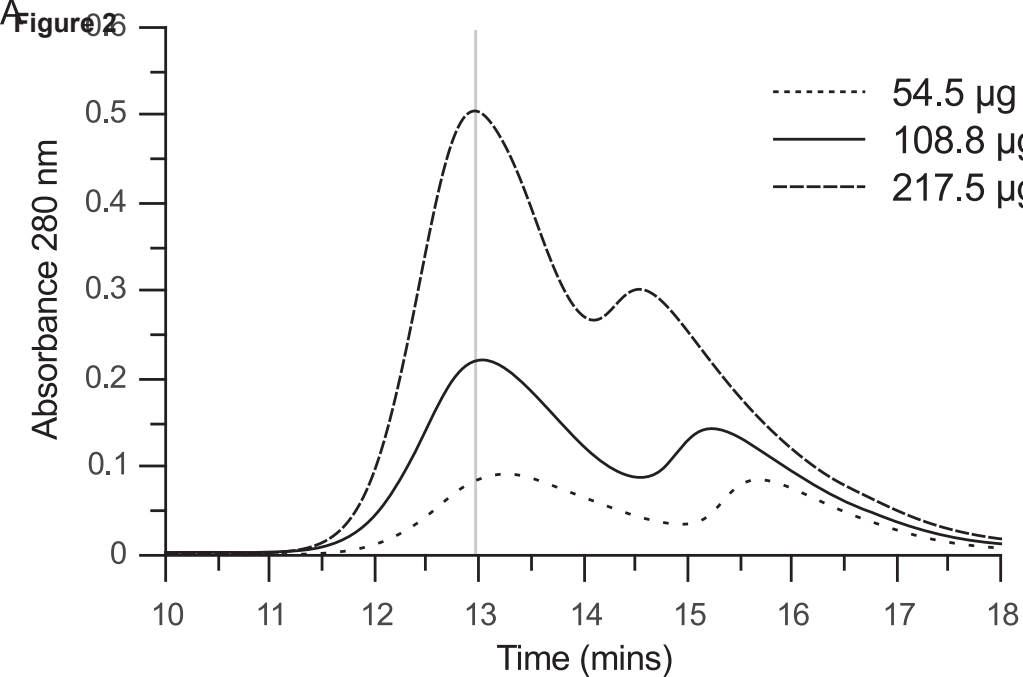
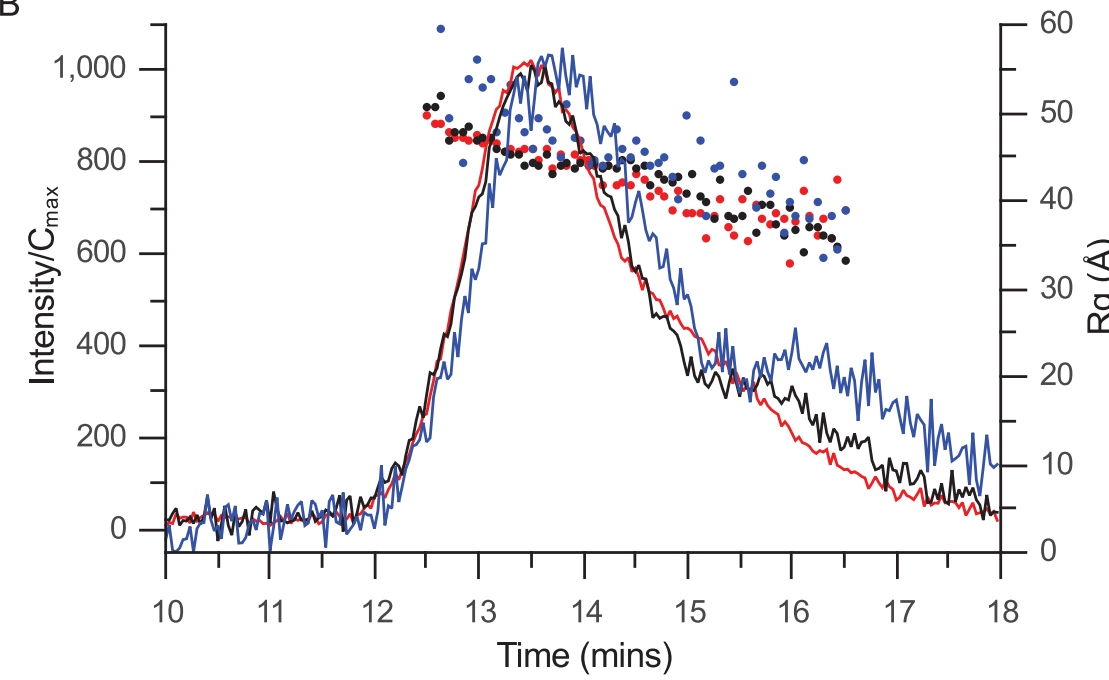
Figure 1

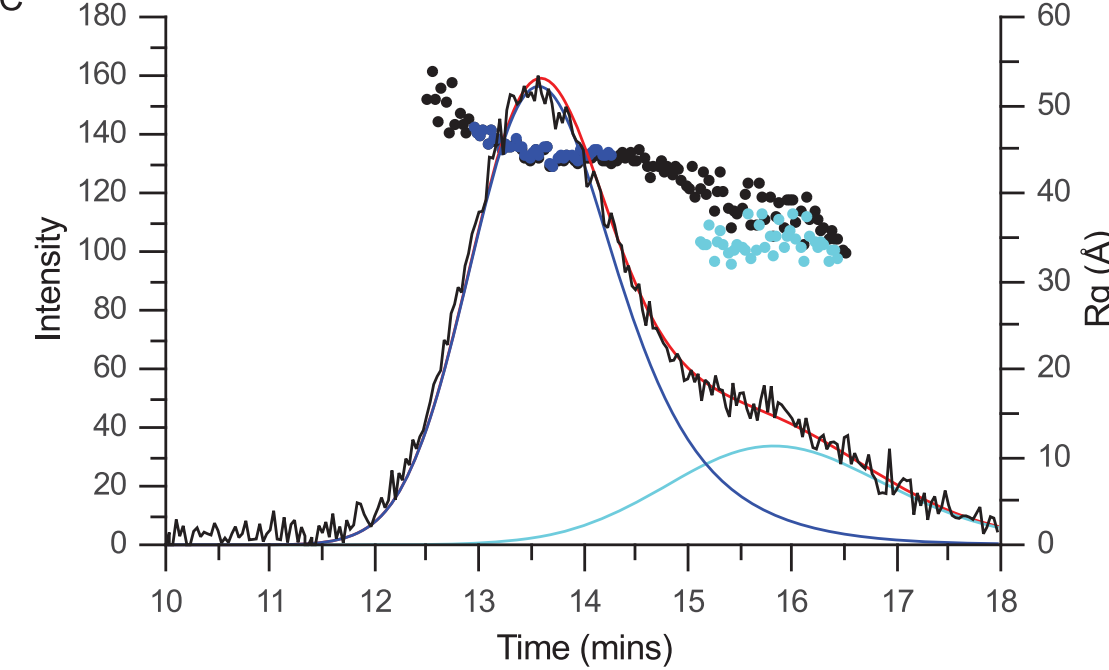
Figure 26



B



C



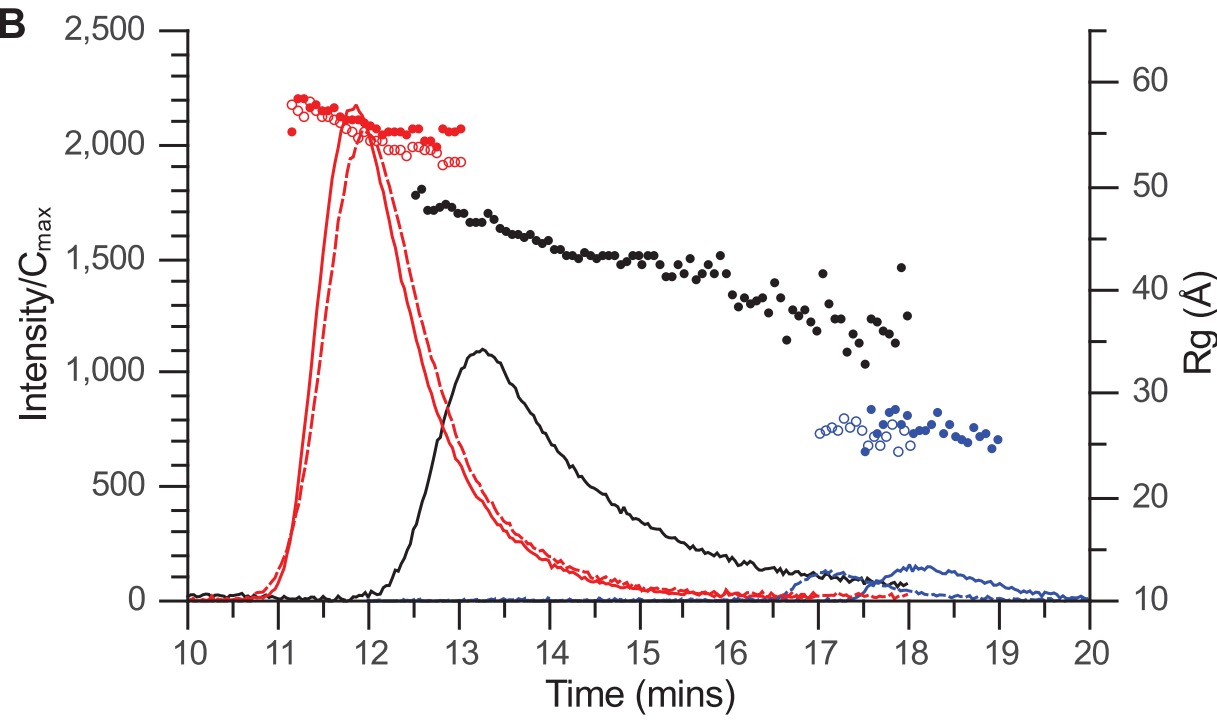
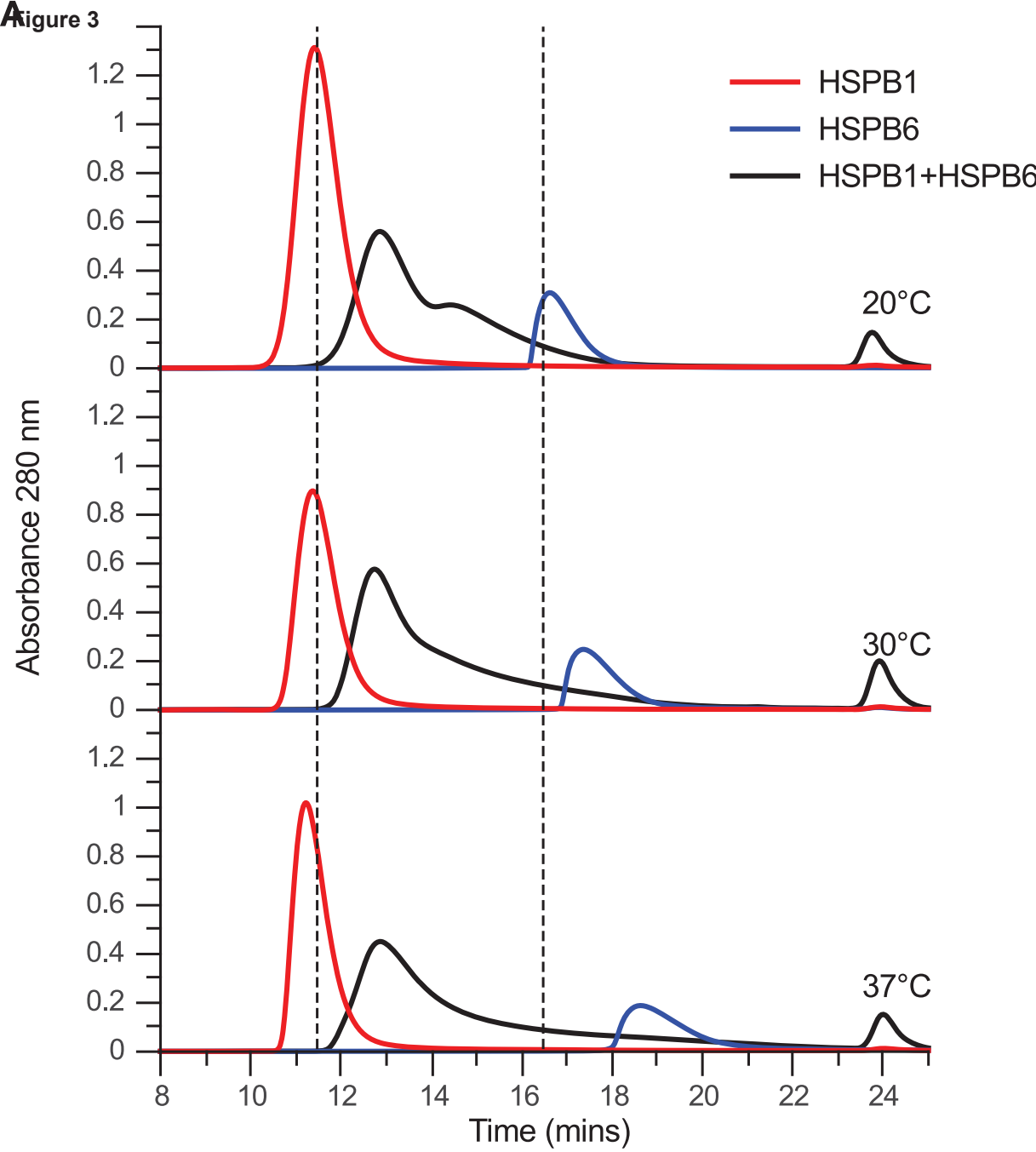


Figure 4

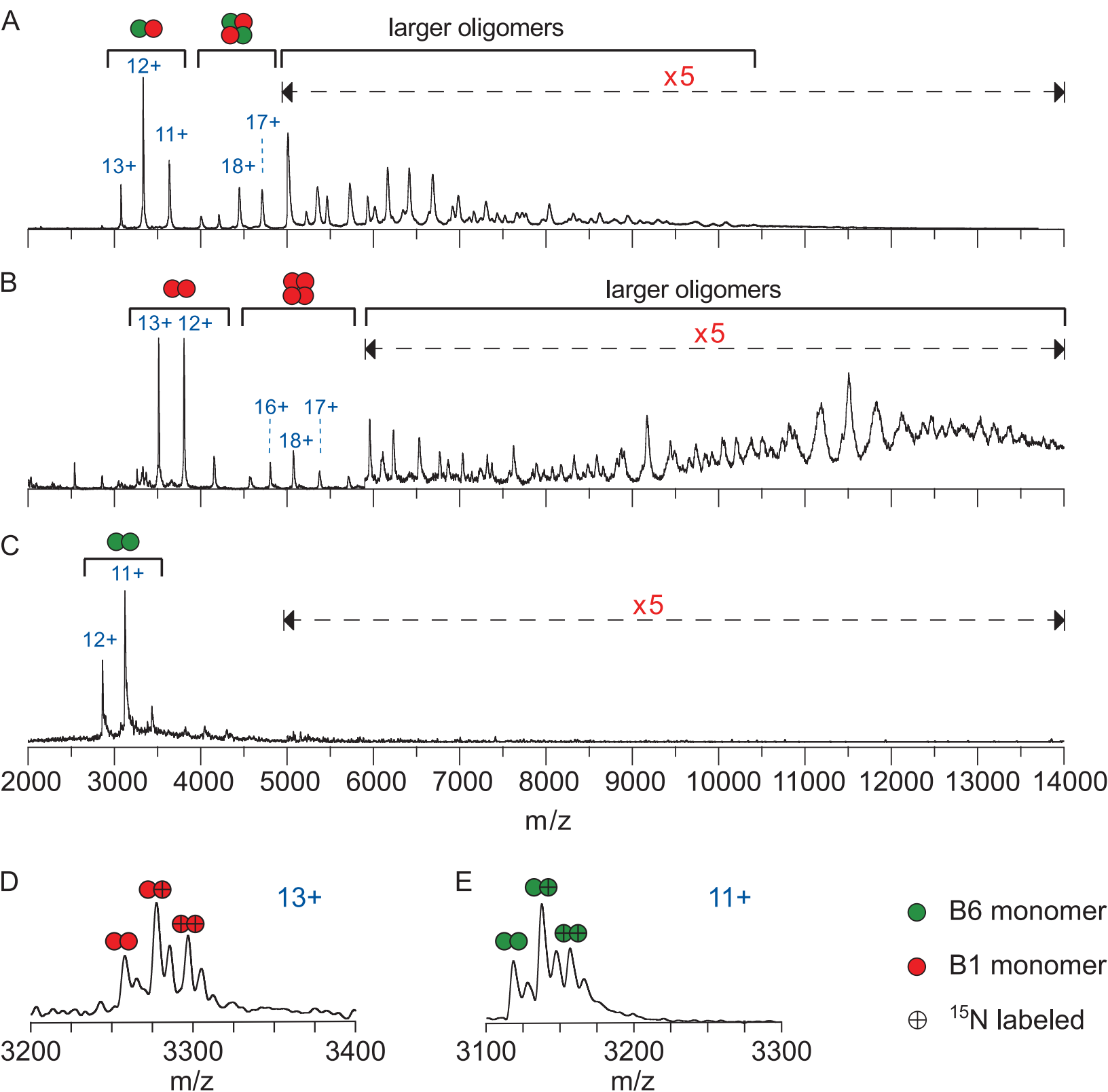


Figure 5

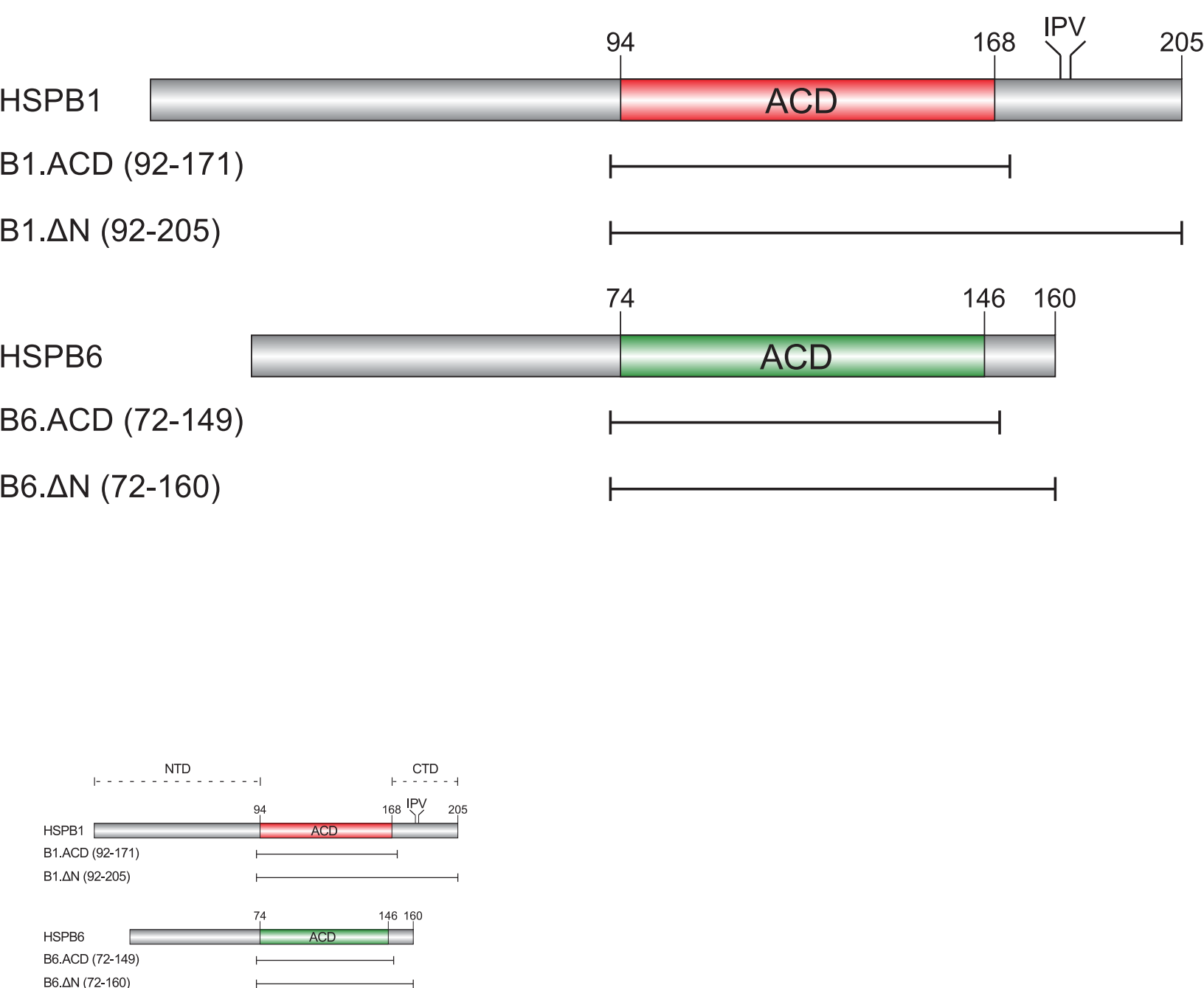


Figure 6

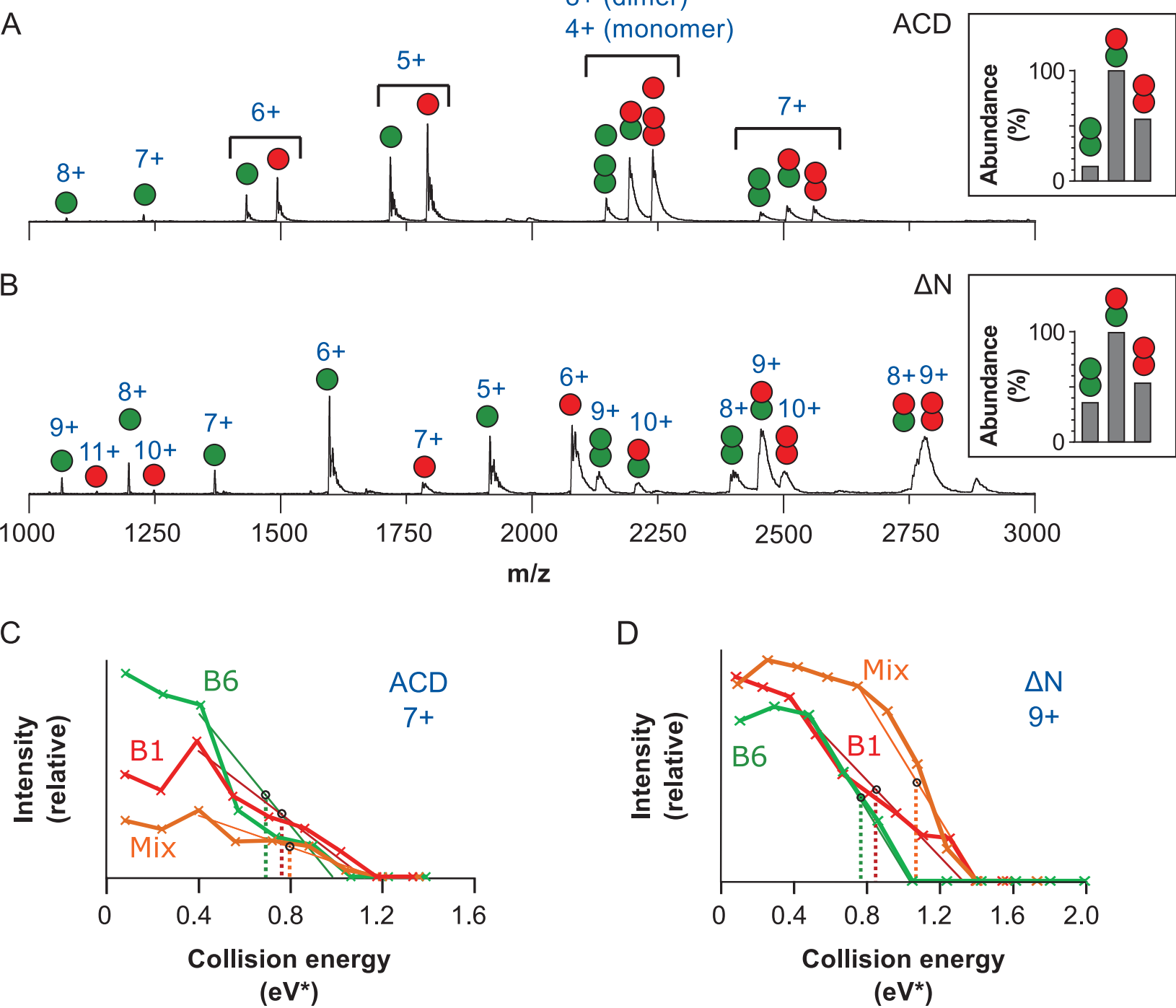


Table 1. Molecular weight estimates of species at the SEC-coupled SAXS scattering maxima.

Temperature (°C)	HSPB1		HSPB6		HSPB1/HSPB6	
	M _r ^a	Subunits	M _r	Subunits	M _r	Subunits ^b
15	540.0	24	37.0	2	258.4	13
20	553.4	24	37.7	2	263.9	13
30	573.3	25	45.8	3	292.2	15
37	643.9	28	38.7	2	293.4	15

^a The molecular weight was calculated from the Q_R value [30], determined from the averaged SAXS scattering curve.

^b An average molecular weight of 20.0 kDa was used for calculation of the number of subunits

Supplementary Material

[**Click here to download Supplementary Material: Supplement_revised_20160913.docx**](#)